

Coordination and solvation of noble metal ions: Infrared spectroscopy of $\text{Ag}^+(\text{H}_2\text{O})_n$

T. Iino¹, K. Ohashi^{1,a}, K. Inoue¹, K. Judai², N. Nishi², and H. Sekiya¹

¹ Department of Chemistry, Faculty of Sciences, Kyushu University, Hakozaki, Fukuoka 812-8581, Japan

² Institute for Molecular Science, Myodaiji, Okazaki 444-8585, Japan

Received 23 July 2006 / Received in final form 30 October 2006

Published online 24 May 2007 – © EDP Sciences, Società Italiana di Fisica, Springer-Verlag 2007

Abstract. Vibrational spectra of mass-selected $\text{Ag}^+(\text{H}_2\text{O})_n$ ions are measured by infrared photodissociation spectroscopy and analyzed with the aid of density functional theory calculations. Hydrogen bonding between H_2O molecules is found to be absent for cold $\text{Ag}^+(\text{H}_2\text{O})_3$, but detected for $\text{Ag}^+(\text{H}_2\text{O})_4$ through characteristic changes in the position and intensity of OH-stretching transitions. The third H_2O coordinates directly to Ag^+ , but the fourth H_2O prefers solvation through hydrogen bonding. The preference of the tri-coordinated form is attributed to the inefficient $5s-4d$ hybridization in Ag^+ , in contrast to the efficient $4s-3d$ hybridization in Cu^+ . For $\text{Ag}^+(\text{H}_2\text{O})_4$, however, di-coordinated isomers are identified in addition to the tri-coordinated one.

PACS. 36.40.Mr Spectroscopy and geometrical structure of clusters – 36.20.Ng Vibrational and rotational structure, infrared and Raman spectra

1 Introduction

The interaction of metal ions with small ligands, e.g. water and ammonia, has been a prototype for considering ion solvation. Gas-phase studies of solvated metal ions have contributed significantly to our understanding of metal–ligand interactions [1]. High-pressure mass spectrometry has been used to obtain the enthalpies and free energies of association as a function of solvent number [2,3]. The metal–ligand binding energies have also been measured in collision-induced dissociation (CID) experiments [4,5]. Recently, infrared (IR) spectroscopy has been applied to the study of gas-phase ions, providing detailed information on the solvation structures [6,7].

The $\text{Ag}^+(\text{H}_2\text{O})_n$ system has received significant experimental and theoretical attention. Holland and Castleman [8] obtained the stepwise binding energies of $\text{H}_2\text{O}\cdots\text{Ag}^+(\text{H}_2\text{O})_{n-1}$ for $n = 1-6$ using high-pressure mass spectrometry. They observed that the first two waters are bound much strongly than the third and further ones. The result was explained in terms of the hybridization of the $5s$ and $4d$ orbitals of Ag, in reference to the common coordination structure of Ag(I) found in inorganic complexes. Theoretical calculations [9–13] have also been carried out for $\text{Ag}^+(\text{H}_2\text{O})_n$ to predict geometrical structures, incremental binding energies, and vibrational frequencies. In particular, special attention has been paid to the coordination number, i.e. the number of ligands bonded directly

to the Ag^+ ion. Fox et al. [12] reported the coordination number of 2 for the lowest-energy forms of $\text{Ag}^+(\text{H}_2\text{O})_{2-4}$ from density functional theory (DFT) calculations. Lee et al. [13] confirmed that the DFT calculations predict the coordination number of 2 for $\text{Ag}^+(\text{H}_2\text{O})_{2-6}$, while the MP2 calculations yield the number of 3 for $\text{Ag}^+(\text{H}_2\text{O})_{3-5}$ and 4 for $\text{Ag}^+(\text{H}_2\text{O})_6$. In this manner, the lowest-energy forms of $\text{Ag}^+(\text{H}_2\text{O})_n$ are sensitive to the method of calculations. IR spectroscopy is a powerful tool for establishing the coordination number, because it is possible to detect the completion of the first solvent shell through the observation of hydrogen bonding between H_2O molecules.

We have reported the IR spectra and solvation structures of hydrated Cu^+ ions [14]. The coordination number of $\text{Cu}^+(\text{H}_2\text{O})_3$ and $\text{Cu}^+(\text{H}_2\text{O})_4$ is confirmed to be 2, where the di-coordinated subunit acts as the core of further solvation processes. In this work, we turn our attention to another metal belonging to the same group. The $5s-4d$ energy gap of Ag is larger than the $4s-3d$ gap of Cu, which is likely to influence the efficiency in the $s-d$ hybridization. We compare the results of $\text{Ag}^+(\text{H}_2\text{O})_n$ with those of $\text{Cu}^+(\text{H}_2\text{O})_n$ for exploring the effect of the electronic structure of the metals on their solvation structures.

2 Experimental and computational

The experiment is performed using a triple quadrupole mass spectrometer equipped with a laser-vaporization ion

^a e-mail: kazu.scc@mbox.nc.kyushu-u.ac.jp

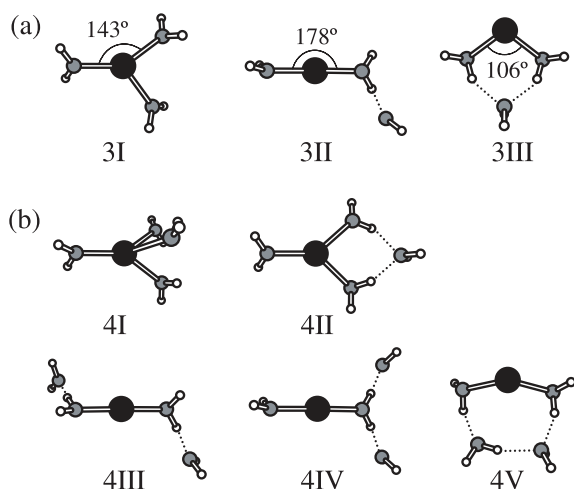


Fig. 1. Stable structures of (a) $\text{Ag}^+(\text{H}_2\text{O})_3$ and (b) $\text{Ag}^+(\text{H}_2\text{O})_4$ obtained from DFT calculations. Ag and O atoms are denoted by solid and shaded circles, respectively.

source [14–16]. $\text{Ag}^+(\text{H}_2\text{O})_n$ and $\text{Ag}^+(\text{H}_2\text{O})_n\cdot\text{Ar}$ ions are mass-selected and probed through IR photodissociation spectroscopy in the region of OH-stretching vibrations. The IR source is an optical parametric oscillator system (Continuum, Mirage 3000). Theoretical calculations are carried out with Gaussian 03 program package [17] using the hybrid DFT method (B3LYP) [18,19] with the relativistic effective core potential [20] for Ag and 631+G(d) for other atoms. The IR spectra of $\text{Ag}^+(\text{H}_2\text{O})_n$ are computed for analyzing the experimental spectra.

3 Results and discussion

3.1 Minimum-energy structures

The geometries of $\text{Ag}^+(\text{H}_2\text{O})_n$ were optimized for $n = 1$ at the HF and MP2 levels by Chattaraj and Schleyer [9], for $n = 1-4$ at the RHF and MP2 levels by Feller et al. [10], for $n = 1$ and 2 at the BP86 and CCSD(T) levels by Widmer-Cooper et al. [11], for $n = 1-4$ at the B3LYP level by Fox et al. [12], and for $n = 1-6$ at the B3LYP and MP2 levels by Lee et al. [13]. Briefly, the oxygen atom of H_2O is bonded to the Ag^+ ion; the main interaction is the charge-dipole attraction between Ag^+ and H_2O . The $5s$ and $4d\sigma$ orbitals of Ag hybridize for reducing the exchange repulsion between the lone pairs of the oxygen atom and $d\sigma$ electrons of Ag^+ . As a result, the second H_2O is located on the side opposite the first, forming a twofold linear coordination. $\text{Ag}^+(\text{H}_2\text{O})_1$ and $\text{Ag}^+(\text{H}_2\text{O})_2$ have coordination structures similar to $\text{Cu}^+(\text{H}_2\text{O})_1$ and $\text{Cu}^+(\text{H}_2\text{O})_2$, respectively.

Figure 1a shows minimum-energy structures of $\text{Ag}^+(\text{H}_2\text{O})_3$ obtained from our DFT calculations. The labeling ($n_1 + n_2$) is used hereafter to classify the solvation structures, where n_1 stands for the coordination number and n_2 is the number of ligands in the second solvation shell. All the three H_2O molecules in 3I are bonded directly to Ag^+ in a (3+0) form. In the process of accom-

modating the third H_2O , the originally linear O–Ag–O angle is reduced to 143° at the cost of the stabilization energy gained through the $5s-4d$ hybridization. In 3II, on the other hand, the twofold linear coordination remains intact and the additional H_2O is hydrogen-bonded to one of the first-shell waters. Since the charge on the Ag^+ ion polarizes the H-donating H_2O in the first shell, the resulting ‘charge-enhanced’ hydrogen bond is substantially strong [21]. The O–Ag–O angle is as small as 106° in 3III, allowing the third H_2O to bridge the first-shell molecules. The formation of double hydrogen bonds stabilizes 3III at the expense of the $5s-4d$ hybridization. The previous theoretical studies showed that the lowest-energy form of $\text{Ag}^+(\text{H}_2\text{O})_3$ is sensitively dependent on the method of calculations. 3I is more stable than 3II by 9 kJmol^{-1} at the CCSD(T)/aug-cc-pVDZ level, although 3I is less stable than 3II by 7 kJmol^{-1} at the B3LYP/aug-cc-pVDZ level [13]. 3III lies $26-31 \text{ kJmol}^{-1}$ higher than the most stable isomer at the MP2 and B3LYP levels [12,13].

Structures 4I–III displayed in Figure 1b are (4+0), (3+1), and (2+2) forms of $\text{Ag}^+(\text{H}_2\text{O})_4$ obtained from our geometry optimization. Other (2+2) forms, 4IV and 4V, are also included here, which are necessary to explain the IR spectrum of $\text{Ag}^+(\text{H}_2\text{O})_4\cdot\text{Ar}$ (see Sect. 3.2). Four H_2O molecules in 4I exhibit a slightly distorted tetrahedral coordination. The fourth H_2O in 4II bridges two of the three first-shell waters through hydrogen bonds. The twofold linear coordination remains intact in the (2+2) forms 4III–V. In 4III, the third and fourth waters are bound to different H_2O in the first shell, while they are bonded to the same H_2O in 4IV. Two additional waters in 4V form the dimer, which bridges the first-shell waters through hydrogen bonds. The lowest-energy structure of $\text{Ag}^+(\text{H}_2\text{O})_4$ is again sensitive to the method of calculations. 4I and 4III lie 3 and 10 kJmol^{-1} above the most stable 4II, respectively, at the CCSD(T)/aug-cc-pVDZ level, while 4I and 4II lie 23 and 10 kJmol^{-1} above the most stable 4III, respectively, at the B3LYP/aug-cc-pVDZ level [13]. 4IV and 4V are less stable than 4III by 14 and 24 kJmol^{-1} , respectively, at the B3LYP level [12,13].

3.2 IR photodissociation spectra

Figure 2 compares the IR photodissociation spectra of $\text{Ag}^+(\text{H}_2\text{O})_3$ and $\text{Ag}^+(\text{H}_2\text{O})_3\cdot\text{Ar}$ with the theoretical spectra of 3I–III. All the theoretical spectra possess weak transitions in the $3600-3750 \text{ cm}^{-1}$ region, which are associated with stretching vibrations of non-hydrogen-bonded, namely, free OH groups. In addition, fingerprint transitions appear at 3168 cm^{-1} for 3II and at 3491 and 3514 cm^{-1} for 3III, which are characteristic of hydrogen-bonded OH groups. Since the linear hydrogen bond in 3II is stronger than the bent ones in 3III, the frequency reduction upon hydrogen bonding is much larger for the 3168 cm^{-1} transition of 3II.

The experimental spectrum of $\text{Ag}^+(\text{H}_2\text{O})_3$ (Fig. 2a) shows broad and strong features extending from 3100 to 3600 cm^{-1} . The appearance of these features is indicative

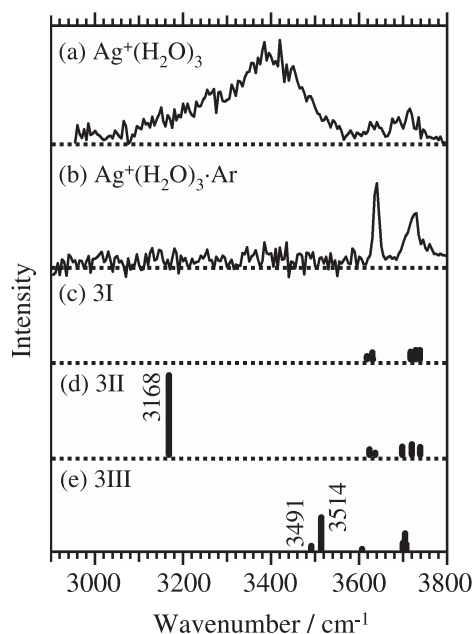


Fig. 2. Comparison of experimental IR spectra of (a) $\text{Ag}^+(\text{H}_2\text{O})_3$ and (b) $\text{Ag}^+(\text{H}_2\text{O})_3\cdot\text{Ar}$ with theoretical IR spectra obtained from DFT calculations for (c) 3I, (d) 3II, and (e) 3III.

of hydrogen bonding between H_2O molecules. The overwhelming intensity of the bonded-OH features suggests that the majority of the $\text{Ag}^+(\text{H}_2\text{O})_3$ ions take the (2+1) form(s) 3II and/or 3III. The broadness of these features can be ascribed to the following fact. The energy of a photon in the $3000\text{--}3800\text{ cm}^{-1}$ region ($35\text{--}45\text{ kJmol}^{-1}$) is smaller than the $\text{H}_2\text{O}\cdots\text{Ag}^+(\text{H}_2\text{O})_2$ bond dissociation energy (63 kJmol^{-1}) [8]. This means that we preferentially detect a subset of the hot ions that have internal energies sufficient to break the $\text{H}_2\text{O}\cdots\text{Ag}^+(\text{H}_2\text{O})_2$ bond following one-photon absorption. These hot ions may not reside near the global minimum on the potential energy surface on average, because large-amplitude intermolecular vibrations must be highly excited. So we carry out the Ar-tagging experiment [22] for reducing the internal energies of the ions. We assume that the $\text{Ag}^+(\text{H}_2\text{O})_3\cdot\text{Ar}$ ions are colder than $\text{Ag}^+(\text{H}_2\text{O})_3$, because nascent hot $\text{Ag}^+(\text{H}_2\text{O})_3\cdot\text{Ar}$ ions are going to decompose by ejecting the weakly bound Ar atom prior to the mass selection. The spectrum of $\text{Ag}^+(\text{H}_2\text{O})_3\cdot\text{Ar}$ is shown in Figure 2b. To our surprise, the bonded-OH features dominating the $\text{Ag}^+(\text{H}_2\text{O})_3$ spectrum disappear completely. The observation implies that the (2+1) forms are missing and only the (3+0) form is populated under cold conditions with Ar-tagging. Therefore, 3I (3+0) is concluded to be the most stable structure of $\text{Ag}^+(\text{H}_2\text{O})_3$, which is consistent with the result of the CCSD(T) calculations [10, 13].

The IR photodissociation spectra of $\text{Ag}^+(\text{H}_2\text{O})_4$ and $\text{Ag}^+(\text{H}_2\text{O})_4\cdot\text{Ar}$ are compared with the theoretical spectra of 4I–V in Figure 3. All the transitions of 4I are associated with the free OH groups. The spectrum of 4II is similar to that of 3III, because the two forms commonly have a double-acceptor H_2O in the second shell. Transitions of

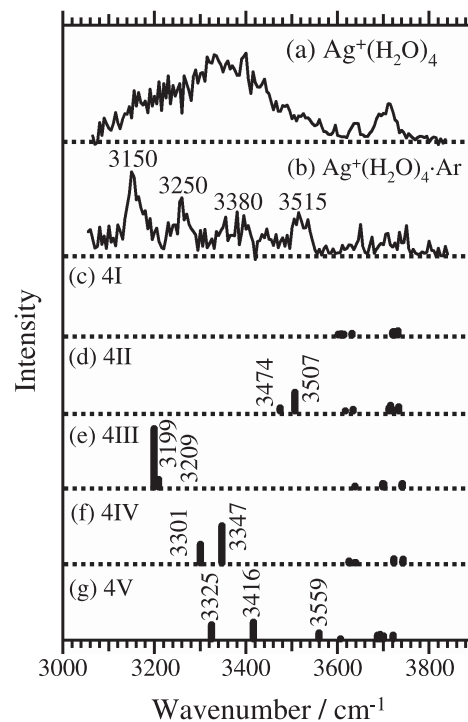


Fig. 3. Comparison of experimental IR spectra of (a) $\text{Ag}^+(\text{H}_2\text{O})_4$ and (b) $\text{Ag}^+(\text{H}_2\text{O})_4\cdot\text{Ar}$ with theoretical IR spectra obtained from DFT calculations for (c) 4I, (d) 4II, (e) 4III, (f) 4IV, and (g) 4V.

the bonded-OH groups in 4III are located at 3199 and 3209 cm^{-1} . The 3301 and 3347 cm^{-1} transitions of 4IV originate from the double-donor H_2O , showing red shifts smaller than the bonded-OH stretches of 4III. Three types of H-donating OH groups are responsible for the transitions located at 3325, 3416, and 3559 cm^{-1} in the spectrum of 4V.

Broad and strong features are observed in the $3100\text{--}3600\text{ cm}^{-1}$ region of the experimental spectrum of $\text{Ag}^+(\text{H}_2\text{O})_4$ (Fig. 3a), indicating that large parts of the $\text{Ag}^+(\text{H}_2\text{O})_4$ ions are hydrogen-bonded isomers under warm conditions. The broad features are to be resolved in the Ar-tagging experiment. The spectrum of $\text{Ag}^+(\text{H}_2\text{O})_4\cdot\text{Ar}$ (Fig. 3b) exhibits at least four distinct bands at 3150, 3250, 3380, and 3515 cm^{-1} in the region of the bonded-OH stretches. The lowest-frequency band at 3150 cm^{-1} is attributable to the 3199 cm^{-1} transition of 4III, while the highest-frequency band at 3515 cm^{-1} can be assigned to the 3507 cm^{-1} transition of 4II. The remaining bands at 3250 and 3380 cm^{-1} may arise from 4IV and/or 4V. It is difficult to ascertain the presence of 4I, because it has no fingerprint transitions below 3600 cm^{-1} . We can estimate that the abundance of 4II (3+1) and 4III (2+2) is comparable with each other, from the integrated intensity of the 3150 and 3515 cm^{-1} bands and the calculated intensity of the 3199 and 3507 cm^{-1} transitions of 4III and 4II, respectively. The coexistence of 4II and 4III under cold conditions signifies that the energy difference between the two forms should be considerably small. The experimental finding is in accord with the results of the

CCSD(T) calculations [13], which predict that the difference in the energies of 4I–III falls within 10 kJmol^{-1} .

3.3 Coordination structures

We have shown that the gas-phase coordination number of Cu^+ in $\text{Cu}^+(\text{H}_2\text{O})_3$ and $\text{Cu}^+(\text{H}_2\text{O})_4$ is 2 as a result of the anomalous stability of the twofold linear coordination [14]. The stability has been ascribed to the $4s$ – $3d$ hybridization of the Cu orbitals [23]. It is generally accepted that the $5s$ – $4d$ hybridization of the Ag orbitals is also important in determining the coordination structures of Ag^+ . If this is the case, $\text{Ag}^+(\text{H}_2\text{O})_3$ should take the (2+1) form rather than the (3+0) form. With regard to theoretical studies, the previous calculations [10, 12, 13] showed that the energy difference between 3I (3+0) and 3II (2+1) is quite small. The present IR spectroscopy with Ar-tagging establishes that the lowest-energy structure of $\text{Ag}^+(\text{H}_2\text{O})_3$ is 3I (3+0). By reducing the O–Ag–O angle to 143° , the $\text{Ag}^+(\text{H}_2\text{O})_2$ subunit allows the third H_2O to coordinate directly to Ag^+ , at the expense of the stabilization through the $5s$ – $4d$ hybridization. Since the $5s$ – $4d$ gap of Ag (6.5 eV) is larger than the $4s$ – $3d$ gap of Cu (4.6 eV) [13, 24], the $5s$ – $4d$ hybridization in Ag is less efficient. Accordingly, the Ag^+ ion can accommodate three ligands in the first shell.

The spectral features change drastically with the temperature of $\text{Ag}^+(\text{H}_2\text{O})_3$. Although the (2+1) forms are completely missing under cold conditions with Ar-tagging, the main features in the spectrum of warm $\text{Ag}^+(\text{H}_2\text{O})_3$ are due to the (2+1) form(s). We expect that the increase in the population of 3II (2+1) is driven entropically, since it is less crammed than 3I (3+0). Consequently, 3II should be observed in warm ions without Ar-tagging.

The most stable form of $\text{Cu}^+(\text{H}_2\text{O})_n$ is approximated by the attachment of the n th H_2O to the most stable form of $\text{Cu}^+(\text{H}_2\text{O})_{n-1}$ [24]. For $\text{Ag}^+(\text{H}_2\text{O})_4$, the present IR spectroscopy reveals the coexistence of the (3+1) and (2+2) forms. The observation of 4II (3+1) is reasonable, because the tri-coordinated 3I is the lowest-energy form of $\text{Ag}^+(\text{H}_2\text{O})_3$. On the other hand, the appearance of the dicoordinated 4III is somewhat surprising. Although the $5s$ – $4d$ hybridization is inefficient in Ag, the formation of two linear hydrogen bonds induces revival of the di-coordinated $\text{Ag}^+(\text{H}_2\text{O})_2$ core. The successive solvation process of $\text{Ag}^+(\text{H}_2\text{O})_n$ is in contrast to that of $\text{Cu}^+(\text{H}_2\text{O})_n$, where the twofold linear coordination remains to be the most stable core from $n = 3$ to at least 6 [24].

This work was supported in part by the Joint Studies Program (2005) of the Institute for Molecular Science and the Grant-in-Aid for Scientific Research (No. 17550014) from the Ministry of Education, Culture, Sports, Science, and Technology (MEXT), Japan.

References

1. A.W. Castleman Jr, K.H. Bowen, *J. Phys. Chem.* **100**, 12911 (1996)
2. P. Kebarle, *Ann. Rev. Phys. Chem.* **28**, 445 (1977)
3. A.W. Castleman Jr, R.G. Keese, *Chem. Rev.* **86**, 589 (1986)
4. P.B. Armentrout, *Acc. Chem. Res.* **28**, 430 (1995).
5. L. Poisson, P. Pradel, F. Lepetit, F. Réau, J.-M. Mestdagh, J.-P. Visticot, *Eur. Phys. J. D* **14**, 89 (2001)
6. J.M. Lisy, *Int. Rev. Phys. Chem.* **16**, 267 (1997)
7. M.A. Duncan, *Int. Rev. Phys. Chem.* **22**, 407 (2003)
8. P.M. Holland, A.W. Castleman Jr, *J. Chem. Phys.* **76**, 4195 (1982)
9. P.K. Chattaraj, P.v.R. Schleyer, *J. Am. Chem. Soc.* **116**, 1067 (1994)
10. D. Feller, E.D. Glendening, W.A. de Jong, *J. Chem. Phys.* **110**, 1475 (1999)
11. A.N. Widmer-Cooper, L.F. Lindoy, J.R. Reimers, *J. Phys. Chem. A* **105**, 6567 (2001)
12. B.S. Fox, M.K. Beyer, V.E. Bondybey, *J. Am. Chem. Soc.* **124**, 13613 (2002)
13. E.C. Lee, H.M. Lee, P. Tarakeshwar, K.S. Kim, *J. Chem. Phys.* **119**, 7725 (2003)
14. T. Iino, K. Ohashi, Y. Mune, Y. Inokuchi, K. Judai, N. Nishi, H. Sekiya, *Chem. Phys. Lett.* **427**, 24 (2006)
15. Y. Inokuchi, N. Nishi, *J. Chem. Phys.* **114**, 7059 (2001)
16. Y. Inokuchi, K. Ohshimo, F. Misaizu, N. Nishi, *Chem. Phys. Lett.* **390**, 140 (2004)
17. M.J. Frisch et al., *Gaussian 03*, Gaussian Inc., Pittsburgh, 2003
18. A.D. Becke, *Phys. Rev. A* **38**, 3098 (1988)
19. C. Lee, W. Yang, R.G. Parr, *Phys. Rev. B* **37**, 785 (1988)
20. D. Andrae, U. Häußermann, M. Dolg, H. Stoll, H. Preuß, *Theor. Chim. Acta* **77**, 123 (1990)
21. A.J. Stace, *Phys. Chem. Chem. Phys.* **3**, 1935 (2001)
22. H. Machinaga, K. Ohashi, Y. Inokuchi, N. Nishi, H. Sekiya, *Chem. Phys. Lett.* **391**, 85 (2004)
23. M. Rosi, C.W. Bauschlicher Jr, *J. Chem. Phys.* **90**, 7264 (1989)
24. H.M. Lee, S.K. Min, E.C. Lee, J.-H. Min, S. Odde, K.S. Kim, *J. Chem. Phys.* **122**, 064314 (2005)